Palaeogeography, Palaeoclimatology, Palaeoecology 683 (2026) 113472

Contents lists available at ScienceDirect

Palaeogeography, Palaeoclimatology, Palaeoecology

journal homepage: www.elsevier.com/locate/palaeo

# Trajectories of reef coral morphological traits during the early Paleogene hothouse reveal the predictive limits of fossil analogues in a rapidly changing climate

Francesca R. Bosellini [a], Luca Mariani [a,*], Andrea Benedetti [b]

[a] Dipartimento di Scienze Chimiche e Geologiche, Università di Modena e Reggio Emilia, Via Campi 103, I-41125 Modena, Italy
[b] Dipartimento di Scienze Naturali, Liceo 'Isabella d'Este', Largo Giovanna Baja 9, I-00019 Tivoli, (RM), Italy

ARTICLE INFO

Editor: L Angiolini

*Keywords:*
Scleractinia
Climate change
Conservation paleobiology
Cenozoic
Mediterranean

ABSTRACT

Ancient coral reefs offer critical perspectives on how reef-building organisms responded to past climatic perturbations. This study examines the morphological responses of reef-dwelling scleractinian corals during the early Paleogene (Paleocene–Eocene) hothouse in the Mediterranean region, encompassing the global reef crisis associated with the Paleocene–Eocene Thermal Maximum (PETM) and the Early Eocene Climatic Optimum (EECO), and the subsequent reef recovery phase. Using the newly compiled PalEoCoralTraits (PECT) dataset, we analyse a suite of morphological traits (colony size, growth form, corallite integration, budding type, corallite size and spacing, and septal number) across reef systems affected by long-term ecological stress and environmental change.

Our results show that coral trait responses to early Paleogene hyperthermals only partially align with those observed in modern corals under current warming. While some traits (e.g., colony size) display resilient patterns, others (e.g., growth form, corallite integration) follow divergent trajectories. Increased branching correlates with the proliferation of mixed siliciclastic–carbonate settings, possibly reflecting adaptations to sedimentation and turbidity in mesophotic environments. Morphological disparity rose from the EECO to the late Eocene, coinciding with global cooling and the diversification of *Symbiodinium* clades, potentially supporting renewed reef development and functional innovation.

Discrepancies between fossil and modern coral responses likely result from differences in the rate and magnitude of warming, the presence of Anthropocene-specific stressors, and variation in data resolution, sampling biases, and preservation quality. The decoupling of coral diversity and reef development in the Paleocene–Eocene further points to distinct boundary conditions or ecological thresholds.

These findings highlight the value of the fossil record for identifying ecological tipping points, recovery dynamics, and trait-based strategies that shaped coral reef persistence under climatic stress.

## 1. Introduction

Modern coral reefs are among the most diverse and valuable ecosystems on the planet, providing habitat for marine life, protecting coastlines, and supporting local economies. However, they are also some of the most susceptible ecosystems, increasingly threatened by climate change, which disrupts their delicate balance (Pandolfi et al., 2003; Hughes et al., 2017a; Eddy et al., 2021). Rising ocean temperatures, acidification, and local stressors such as pollution and overfishing are severely impacting reefs worldwide, with predictions suggesting they could face near-total collapse by the end of the century under extreme global warming scenarios (Hoegh-Guldberg et al., 2007; Hughes et al., 2017b; IPCC, 2022). As a consequence, the corals that construct these vital ecosystems are believed to be at heightened risk of extinction due to climate change (Carpenter et al., 2008), and assessing the vulnerability of different coral species to extinction or, in general, to climate-related stressors is thus a key objective in efforts to protect reef ecosystems.

One of the possible ways to achieve this goal is to examine coral traits, i.e., a suite of physiological, morphological, ecological, phylogenetic, and biogeographic characteristics that are strongly linked to an organism's function, fitness, and response to environmental

* Corresponding author.
*E-mail address:* luca.mariani@unimore.it (L. Mariani).

https://doi.org/10.1016/j.palaeo.2025.113472
Received 21 July 2025; Received in revised form 1 December 2025; Accepted 1 December 2025
Available online 2 December 2025

disturbances (Madin et al., 2016). These traits are now compiled in a single repository, the Coral Trait Database (Madin et al., 2016). Several studies on modern coral reef ecosystems have shown that specific traits determine coral performance, their influence on the environment, and their responses to environmental and anthropogenic stressors (Madin et al., 2016; Denis et al., 2017; Fontoura et al., 2020). Identifying traits that are comparable across taxa and linked to multiple biological and ecological processes provides a useful framework for uncovering the causal relationships between human activities and changes in ecosystem functionality (Zawada et al., 2019). Life-history strategies (competitive, weedy, stress-tolerant, generalist) have been inferred from trait-based classifications, offering insights into species' responses to environmental disturbances (Darling et al., 2012), while spatial and life-history traits have also been related to coral extinction risk and IUCN Red List categories (van Woesik et al., 2012). Considering the potential of trait-based analyses for understanding the dynamics of modern coral reef ecosystems, extending this approach to the geological record is crucial for reconstructing coral community and ecosystem responses over longer timescales, particularly during intervals of elevated global temperatures and major environmental and climatic perturbations (Pandolfi and Kiessling, 2014; Dee et al., 2019; Tierney et al., 2020).

From a geological perspective, the trait-based approach has recently been extended to the fossil record, focusing on preserved skeletal (morphological) rather than biological traits. Similar to the Coral Trait Database for modern corals (Madin et al., 2016), a corresponding repository for fossil taxa, the Ancient Reef Traits Database (ARTD), has been established (Raja et al., 2022). This approach has been used to assess extinction risk by comparing traits of Caribbean corals from the Pliocene–Pleistocene extinction with those of their modern counterparts (van Woesik et al., 2012; Raja et al., 2021). More recently, Dimitrijević et al. (2023) employed ARTD data, particularly corallite diameter, to show that photosymbiotic efficiency increased through the evolutionary history of scleractinian corals from the Middle Triassic to the Holocene. Trait-based comparisons have also been extended to extinct tabulate corals to explore functional diversity linked to the Late Devonian reef collapse (Bridge et al., 2022).

In this study we apply the trait-based approach deeper in time to test its applicability at the geological time scale. The selected time interval is the early Paleogene, that was characterised by some major abrupt warming events such as the hyperthermal Paleocene-Eocene Thermal Maximum (PETM), the Early Eocene Climatic Optimum (EECO), and the Middle Eocene Climatic Optimum (MECO), with the PETM commonly serving as a geologic analogue to anthropogenic warming (McInerney and Wing, 2011).

The PETM, occurring around 56 million years ago and lasting ~170,000 years, was marked by a major disruption of the carbon cycle and a sharp global temperature rise, with estimates ranging from 25.2 °C (Scotese et al., 2021) to 31.6 °C (Inglis et al., 2020), compared to today's 15 °C. The EECO, between 53.3 and 49.1 Ma (Ypresian), represented a prolonged interval of elevated temperatures, with global averages of about 25–27 °C (Scotese et al., 2021; Inglis et al., 2020), accompanied by high atmospheric $CO_2$ levels (Rae et al., 2021). The MECO, lasting ~300,000 years during the Bartonian (40.51–40.21 Ma), temporarily interrupted the overall Eocene cooling trend, raising global temperatures to approximately 23 °C (Scotese et al., 2021).

As regards coral reef ecosystems, the early Paleogene represents a very critical time interval as evidenced by a global collapse of coral reefs (Kiessling and Simpson, 2011; Scheibner and Speijer, 2008; Zamagni et al., 2012). This decline has been linked to a combination of rising sea temperatures and ocean acidification linked to the PETM hyperthermal event. This event had a major effect on coral reef growth and likely promoted the spread of marginal environments where corals had a restricted ability to build reef structures (Scheibner and Speijer, 2008; Zamagni et al., 2012). This crisis, however, did not have a negative impact on coral diversity, which had undergone little significant changes and remained more or less stable throughout the late Paleocene and early Eocene (Simpson et al., 2011; Weiss and Martindale, 2019).

Our analysis is focused on the early Paleogene (Paleocene and Eocene epochs) coral record of the Mediterranean, that has been investigated recently by the creation of an extensive compilation (the PalEoCoral dataset) in order to analyse diversity patterns and their mutual relationship with coral reef development (Benedetti et al., 2024a; Bosellini et al., 2025). During the Paleogene, the Mediterranean region represented a distinct coral province, much like the modern Caribbean and Indo-Pacific provinces. At that time, all three regions were linked through the westward-flowing Tethyan seaway. Notably, the Mediterranean served as the global hotspot for marine biodiversity in the early Paleogene (Renema et al., 2008; Yasuhara et al., 2022). This region boasts an exceptional abundance of Paleogene coral reef sites and fossil collections, extensively studied since the 19th century. As a result, it offers for the early Paleogene a more continuous and complete fossil record compared to the more fragmented histories of the Caribbean and Indo-Pacific.

According to the recent study of Bosellini et al. (2025), the Mediterranean record shows the same decoupling between coral diversity and reef development already identified at the global scale. Coral diversity increased rapidly in the aftermath of the PETM and remained high throughout the Eocene. In contrast, Mediterranean data highlight that reef construction experienced a profound crisis after the PETM, and longer than previously documented: minimum values of reef volume have been reached in the Lutetian and returned to late Paleocene levels by the late Eocene (Bosellini et al., 2025). These findings show that reef corals exhibited a strong resilience in warm climate conditions, whereas coral reefs themselves were much more vulnerable and needed significantly more time to recover.

Based on this picture, that depicts the Mediterranean region as an ideal setting where to test the trait-based approach, we used here the PalEoCoral dataset as a solid starting point. Collecting data about a suite of macromorphological characters such as growth form, corallite integration (a term referring to the structural and morphological connection among corallites, and therefore appropriate for fossil corals; in contrast, "colony integration" describes functional and physiological connectivity, and is more suitable for living corals), corallite size and others, we aim to investigate how these traits changed during the early Paleogene. In particular we aim to detect if those coral morphological traits, that are known as more or less vulnerable to climatic stressors today, have changed accordingly also in the past or responded to different cause-effect mechanisms.

## 2. Material and methods

### 2.1. Data

For this study, we started from the PalEoCoral dataset, a comprehensive compilation that collects data about occurrences of reef corals (i.e., colonial zooxanthellate corals) at both genus and species level for the Mediterranean region and provides updated information about the locality, age and palaeoenvironment for each coral occurrence (Benedetti et al., 2024a; Bosellini et al., 2025). Data have been collected from three different sources: published literature, studies of coral collections in museums (e.g., Bosellini et al., 2022), and also our own collections. For more details about the PalEoCoral dataset we refer to Benedetti et al. (2024a), and to Bosellini et al. (2024a, 2025).

We examined all the references and all the collections included in PalEoCoral and created a new dataset, named PalEoCoralTraits (acronym: PECT) (Table S1). This dataset, composed of 1293 occurrences, includes all the occurrences for which it was possible to extract information about traits from the literature, and all the occurrences related to the analysis of coral collections. Detailed information about the examined collections is available in the PECT dataset.

The macromorphological traits that we selected for this study are the following: colony size, colony growth form (i.e., degree of branching),

colony type (i.e., corallite integration), budding type, corallite size, corallite spacing (CS), distance between corallite centres (CC), and number of septa (NS).

Data about colony size include the maximum width and the maximum height (in cm). They have been extracted from literature when available, both in the case that they were indicated in the description of the specimens or obtained from the analysis of the images in the plates (with scale bar). As regards the collections, for all the specimens we measured the maximum width and the maximum height; fragments of the coral colonies were not considered.

Following Raja et al. (2021, 2022), corallite integration is associated with the arrangement of corallites in a colony, whereas the degree of branching is linked to the colony growth form. Both these traits include a suite of different categories to which we attributed a numerical value (Table S2).

As regards corallite size, the trait is usually expressed by the corallite diameter in corals with monocentric to polycentric corallites, and by the valley width in meandroid corals. In this study we examined the average value of the corallite size for each occurrence. For the collections, we calculated the average of the measurements, made with the calliper or using the micrometre of the microscope, of different (4–5) corallites in the same specimen, with at least two measurements (maximum and minimum diameter) for each corallite or valley. The same for other morphometric characters (CS and CC); the number of septa instead has been counted but with the average calculated in the same way. For the literature we used the data about corallite size indicated in the description of the taxa, or we obtained them from the plates as we did for the colony size.

The descriptions of all the traits considered in this study, included the associated categories, and details about their measurements are summarized in Table S2.

Herein, we also grouped all the specimens of the same species and of the same locality, having the same growth form (as other non-morphometric characters remain the same) into a single occurrence for the entire dataset, calculating the mean values of the morphometric traits. We made this choice in order to solve in part the bias represented by sampling, with localities (and associated collections) extremely rich in coral specimens and oversampled with respect to others. This is the case, for example, of the hotspot recorded from the early-middle Eocene of Friuli in NE Italy where a total of 37 genera and 103 species have been reported (Bosellini et al., 2022).

Our dataset also benefits from an accurate stratigraphic resolution. The age of the coral occurrences considered in this study has been checked and revised for the PalEoCoral dataset based on the Shallow Benthic Zones of larger foraminifera (sensu Serra-Kiel et al., 1998), recently recalibrated for the Paleocene (e.g., Serra-Kiel et al., 2020; Papazzoni et al., 2023) and Eocene intervals (e.g., Luciani et al., 2020; Benedetti et al., 2024b), which allowed a precise stage-level dating of coral deposits (Benedetti et al., 2024a; Bosellini et al., 2025), something not always achievable in shallow-water environments.

Similarly to Bosellini et al. (2025), here we subdivide the investigated interval in seven temporal bins: 1) Danian; 2) Selandian-Thanetian; 3) early Ypresian (Ilerdian); 4) late Ypresian (Cuisian); 5) Lutetian; 6) Bartonian; 7) Priabonian. Although the subdivision of the Paleocene into three stages has been officially recognized since 1989, the Selandian was historically often considered part of the lower Thanetian (e.g., Speijer et al., 2020). As a consequence, the stratigraphic resolution of most published data covering the middle to late Paleocene is affected by inconsistent stratigraphic frameworks. Thus, the Selandian and Thanetian have been combined into a single time interval. As regards the lower Eocene, specifically the Ypresian, to better capture the response of reef corals to the PETM and EECO events, we subdivided this stage into two bins, aligning with the regional stages Ilerdian (representing the lower Ypresian) and Cuisian (representing the upper Ypresian), which are still commonly used for central-western Neotethys shallow-water biostratigraphy (Serra-Kiel et al., 2020; Benedetti et al., 2024a, 2024b).

In order to assess a possible correlation between coral traits and type of reef depositional setting and associated sediment, we examined in detail the literature about the Paleocene and Eocene reef localities of the investigated region and assigned each of them to the category carbonate (C) or mixed carbonate-siliciclastic (M). A cross-check has been made also with the PBDB database where this type of information is directly available (Table S3).

### 2.2. Data analysis

Morphological trait data were statistically analysed throughout the entire database. The analyses focused primarily on descriptive statistics, which were computed separately for each morphological trait and for each temporal bin. For continuous variables, median values and interquartile ranges (IQR), as well as means and standard deviations, were calculated. For categorical variables, relative frequency distributions were assessed. In addition to descriptive analyses, correlation analyses were performed by means of Pearson's r and Spearman's rho (less sensitive to outliers and data far from normal distribution) to explore potential relationships both among different morphological traits and between traits and other variables (e.g., reef-building capacity, sea surface temperature, reef depositional settings, coral diversity). These analyses aimed to investigate potential ecological or environmental controls on traits distribution through time.

## 3. Results

### 3.1. Composition of the dataset

The PECT dataset (Table S1; Fig. 1) includes a total of 1293 coral occurrences, with a nearly balanced contribution from those derived from the studied collections (689 occurrences, 53.3 % of the dataset, about 1256 specimens) and those extracted from literature sources (604 occurrences, 46.7 %). Among the various documented morphological traits, colony type (corallite integration, CI) and budding type (budding value, BV), are the most comprehensively represented, both assessed across the entire dataset. Colony growth form (and consequently the degree of branching, DB) was evaluated for 982 occurrences (76 % of the dataset), whereas the remaining 24 % could not be assessed due to insufficient morphological information in the literature sources or because the available material consisted of fragments lacking diagnostic features. Measurements of colony width and height (colony size) are available for approximately 35 % of the occurrences. Corallite size was recorded in 692 occurrences (53.5 %), whereas other morphological traits have been evaluated for less than 50 % of the occurrences, such as the number of septa (41 %), the C–C distance (33.6 %) and the corallite spacing (15.3 %). Notably, certain traits cannot be measured in all the occurrences. For instance, corallite spacing is not applicable in colonies where corallites are contiguous (e.g., cerioid forms), and in other cases, data were not reported in the literature. Overall, the frequency of the morphological traits within the PECT dataset is uneven, reflecting the limitations due to incomplete descriptions and/or to poorly preserved specimens.

### 3.2. Traits analyses

The results of the statistical analyses performed for each morphological trait across all temporal bins are summarized below:

*Colony size* (Fig. 2). Colony size is represented by measurements of colony width and colony height. For each temporal bin, the median values of both dimensions were calculated, revealing similar trends across all bins. The highest median values occur in the Danian, with colony width and height reaching 11.3 cm and 12.0 cm, respectively. These values decline during the Selandian-Thanetian interval and reach their lowest value in the early Ypresian (Ilerdian), immediately after the

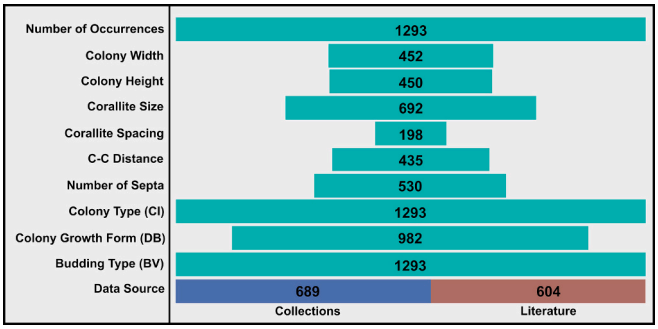


**Fig. 1.** Composition of the PECT dataset. The chart shows the number of data entries available for each morphological trait included in the dataset. The bottom row indicates the source of the data, distinguishing between occurrences from museum collections (689 entries) and records obtained from the scientific literature (604 entries). C–C Distance: Distance between corallite centers; CI: Corallite Integration; DB: Degree of Branching; BV: Budding Value.

PETM. Subsequently, colony size shows a gradual increase, culminating in the Priabonian, where the median colony width and height reach 10.0 cm and 5.0 cm, respectively. It is important to note that while the data from the late Ypresian (Cuisian) to the Priabonian intervals are sufficient for robust statistical interpretation, the number of measurements in the earlier intervals (Danian to Ilerdian) is limited and may be influenced by sampling bias.

*Colony growth form (degree of branching)* (Fig. 3). Colony growth form was assessed for each temporal bin. Massive colonies (DB = 1) consistently represent the most abundant growth form throughout the entire record, accounting for over 40 % of the coral occurrences in all bins and peaking at 50 % in abundance during the Danian. Tabular, platy and encrusting forms (DB = 2) are generally less abundant, but exhibit notable fluctuations. Their relative abundance increases from the Danian to the early Ypresian, reaching a post-PETM maximum of approximately 28 %. This is followed by a decline to below 20 % in the late Ypresian, coinciding with the EECO. Although their abundance increases again in the Lutetian, it remains below pre-EECO levels, stabilizing around 15–20 % until the Priabonian. Branching phaceloid and columnar colonies (DB = 3) are generally the least represented across the dataset, except for the Danian, in which they constitute the 20 % of the occurrences. Their abundance steadily declines to a minimum of ~5 % in the Lutetian, after the EECO. A moderate recovery is observed in the Bartonian and Priabonian, though their relative abundance remains below 20 %. Branching colonies (DB = 4) account for 18 % of the occurrences in the Danian and maintain relatively stable proportions until the late Ypresian, when they peak at approximately 30 % during the EECO. From the Lutetian to the Priabonian, their abundance remains comprised between 22 % and 28 %, consistently higher than pre-EECO levels. The mean DB value was also calculated for each time interval: it reaches a maximum during the late Ypresian (2.23), declines during the Lutetian (2.03) and increases again after the MECO, reaching 2.26 in the Bartonian and 2.28 in the Priabonian.

*Colony type (corallite integration)* (Fig. 4). Colony type was assessed for all the occurrences across each temporal bin in the dataset. Dendroid colonies (CI = 1) are nearly absent, appearing only in the Selandian/Thanetian interval with a relative abundance of 3 %. Phaceloid and, to a lesser extent, reptoid colonies (CI = 2) are generally not abundant throughout the dataset. They account for 17.5 % in the Danian, increase slightly in the Selandian/Thanetian (19 %), and decline gradually to a minimum of 6 % in the Lutetian, before rising again to approximately 13.5 % in both the Bartonian and Priabonian. Plocoid colonies (CI = 3) are consistently abundant throughout all time bins. They comprise 35 % of the occurrences in the Danian, decline slightly to 27 % by the early Ypresian, and then gradually increase to a peak of 42 % in the Priabonian. Cerioid colonies (CI = 4) are also well represented, increasing from 33 % in the Danian to 45 % in the early Ypresian. During the EECO, their relative abundance declines sharply to 28 % in the late Ypresian and 25 % in the Lutetian. After the MECO, cerioid colonies rebound slightly to 32 % in the Bartonian, then decline again to 26 % in the Priabonian. Thamnasterioid colonies (CI = 5) are consistently rare, reaching their highest relative abundances during the late Ypresian (4.7 %) and Lutetian (4 %). Meandroid, hydnophoroid and flabelloid colonies (CI = 6) are widely distributed through each temporal bin, though their relative abundance fluctuates considerably. They constitute the 12 % of the occurrences in the Danian, drop to less than 10 % in the Selandian/Thanetian, then increase steadily reaching a maximum in the Lutetian (32 %). After the MECO, their relative abundance declines to 17 % in the Bartonian and to 18 % in the Priabonian. The mean CI value has been calculated for each temporal bin: after reaching a minimum during the Selandian/Thanetian (3.4), CI increases steadily until a maximum of 4.3

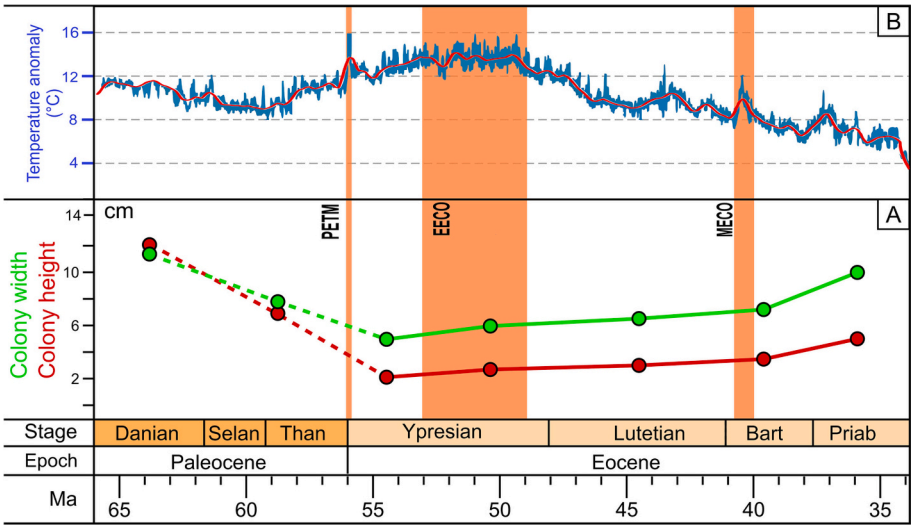


**Fig. 2.** Changes in colony size (green: colony width; red: colony height) of reef corals across the Paleocene and Eocene. A) Median colony width (green) and colony height (red) across Paleocene–Eocene stages. Dashed lines indicate time intervals with low sample size. B) Deep-sea benthic foraminiferal oxygen isotope-derived temperature anomaly (°C) from Westerhold et al. (2020), with the red line showing the smoothed trend. Hyperthermal and warming events are highlighted: PETM (Paleocene-Eocene Thermal Maximum), EECO (Early Eocene Climatic Optimum), and MECO (Middle Eocene Climatic Optimum). (For interpretation of the references to colour in this figure legend, the reader is referred to the web version of this article.)

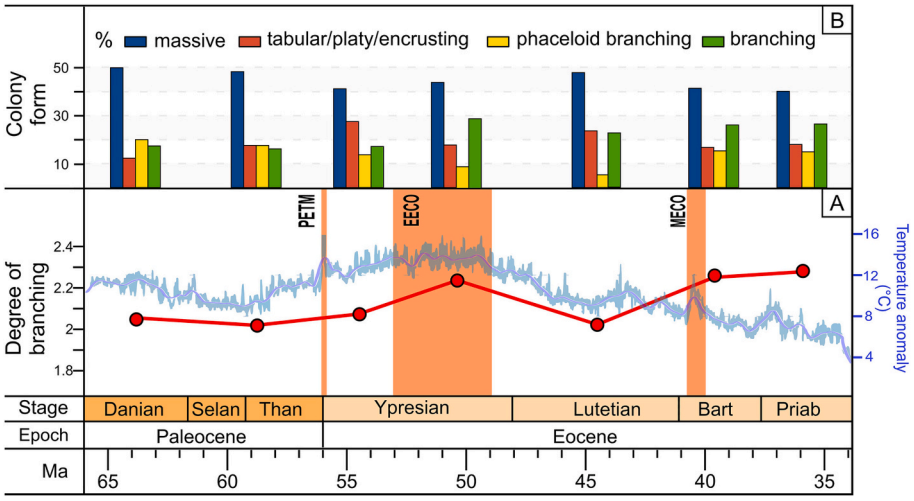


**Fig. 3.** Changes in coral colony form and degree of branching (DB; red line with circles) across the Paleocene and Eocene. A) Degree of branching plotted against global temperature anomaly (blue line; from Westerhold et al., 2020). B) Relative abundance (%) of colony forms across stages. Hyperthermal and warming events are highlighted: PETM (Paleocene-Eocene Thermal Maximum), EECO (Early Eocene Climatic Optimum), and MECO (Middle Eocene Climatic Optimum). (For interpretation of the references to colour in this figure legend, the reader is referred to the web version of this article.)

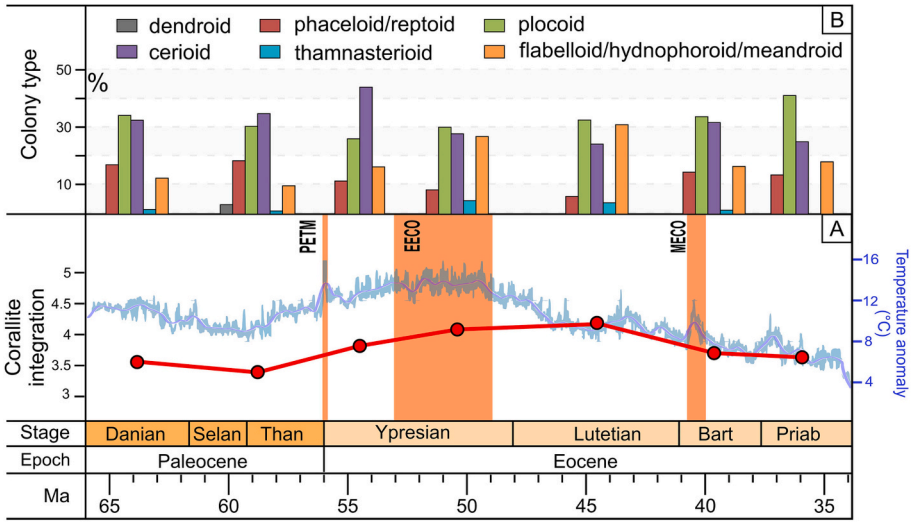


**Fig. 4.** Changes in coral colony type and corallite integration across the Paleocene and Eocene. A) Corallite integration (CI; red line with circles) plotted against global temperature anomaly (blue line; from Westerhold et al., 2020). B) Relative abundance (%) of coral colony types across stages. Hyperthermal and warming events are highlighted: PETM (Paleocene-Eocene Thermal Maximum), EECO (Early Eocene Climatic Optimum), and MECO (Middle Eocene Climatic Optimum). (For interpretation of the references to colour in this figure legend, the reader is referred to the web version of this article.)

in the Lutetian and then declines to 3.6 by the Priabonian. This trait shows a negative correlation (Spearman rho = −0.89, $p = 0.023$) with the reef volume. CI is also negatively correlated with budding type (Pearson $r = -0.94$, $p = 0.0015$; rho = −0.86, $p = 0.024$).

*Budding type* (Fig. 5). Budding type was evaluated for all occurrences across temporal bins, distinguishing between intracalicular (BV = 1) and extracalicular (BV = 2) budding strategies. Extracalicular colonies consistently dominate the dataset across all intervals. Intracalicular colonies represent the 27 % in the Danian, decrease to 20 % in the Selandian/Thanetian, and then increase steadily up to 47 % in the Lutetian. After the MECO, their relative abundance declines to 32 % in the Bartonian and rises slightly to 36 % in the Priabonian. Conversely, extracalicular colonies reach their highest relative abundance in the Selandian/Thanetian (80 %), followed by a gradual decline to 53 % in the Lutetian. Their abundance increases again after the MECO, reaching 68 % in the Lutetian and 64 % in the Priabonian. The mean BV reflect these patterns, peaking at 1.8 in the Selandian/Thanetian, decreasing to 1.5 in the Lutetian, rising again to 1.7 in the Bartonian, and slightly declining to 1.6 in the Priabonian. Budding type is negatively correlated to corallite integration (rho = −0.86, p = 0.024), degree of branching ($r = -0.92$, $p = 0.003$; rho = −0.82, p = 0.023) and corallite size (rho = −0.82, $p = 0.034$).

*Corallite size* (Fig. 6A). Corallite size shows distinct temporal trends in its median values. The median corallite diameter decreases from 3.5 mm in the Danian to a minimum of 2 mm in the Selandian/Thanetian interval. It then increases to 3.8 mm in the early Ypresian, after the PETM, and gradually declines to 2.6 mm in the Lutetian. After the MECO, the median corallite size rises again to 3.4 mm in the Bartonian and remains relatively stable through the Priabonian (3.3 mm). The variability around median values, expressed as the interquartile range (IQR), is highest during the Bartonian and Priabonian. Notably, this variability does not correlate with the number of occurrences measured in each interval, but it is directly correlated with the specific (rho = 0.93, $p = 0.0048$) and generic (rho = 0.86, $p = 0.018$) diversity.

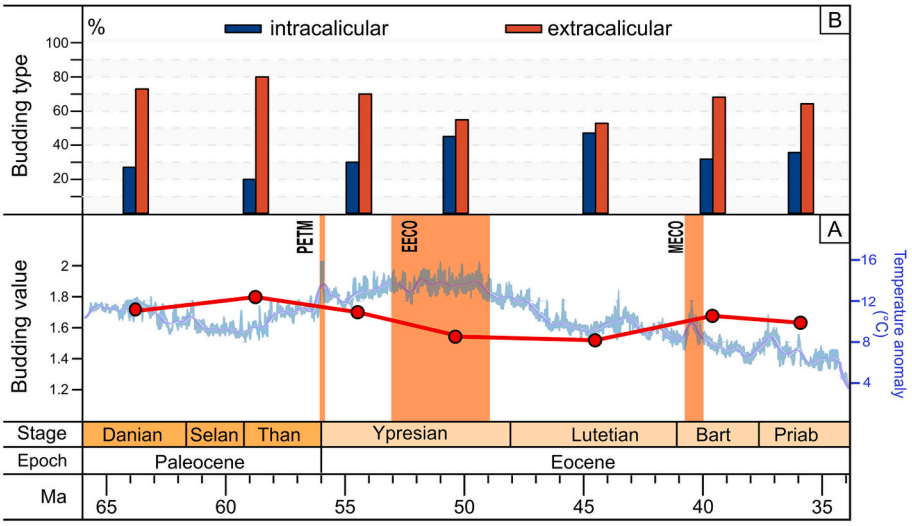


**Fig. 5.** Changes in coral budding type and budding value across the Paleocene and Eocene. A) Budding value (BV; red line with circles) plotted against global temperature anomaly (blue line; from Westerhold et al., 2020), B) Relative abundance (%) of intracalicular and extracalicular colonies across stages. Hyperthermal and warming events are highlighted: PETM (Paleocene-Eocene Thermal Maximum), EECO (Early Eocene Climatic Optimum), and MECO (Middle Eocene Climatic Optimum). (For interpretation of the references to colour in this figure legend, the reader is referred to the web version of this article.)

*Corallite spacing* (Fig. 6B). Corallite spacing exhibits a peak median value of 4.8 mm in the early Ypresian, after the PETM. However, this value is based on a limited number of specimens and may be subject to sampling bias. Excluding this peak, corallite spacing remains relatively stable across the remaining time intervals, with median values ranging from a minimum of 1.2 mm in the Lutetian to a maximum of 2 mm in the Priabonian. Similar to corallite size, the interquartile range indicates greater variability in the Bartonian and Priabonian intervals compared to earlier stages.

*Distance between corallite centres* (Fig. 6C). Corallite centre-to-centre distance (C–C distance) exhibits a trend broadly comparable to that of corallite size. The highest median value is observed in the early Ypresian (4.1 mm), after the PETM; however, even in this case this estimate is based on a limited number of occurrences and may be affected by sampling bias. The C–C distance decreases to 2.4 mm in the late Ypresian, then increases steadily, reaching 3.8 mm in the Bartonian, before declining slightly to 3 mm in the Priabonian. Similarly to other morphological traits, the interquartile range is notably higher during the Bartonian and Priabonian intervals compared to earlier stages.

*Number of septa* (Fig. 6D). The number of septa shows a fluctuating trend in its median values over time. The median number of septa increases from 22 in the Danian to 24 in the early Ypresian, after the PETM. A marked decline occurs in the late Ypresian, where the median drops to 18, remains relatively stable until the Bartonian (19), before rising again to 24 in the Priabonian. In this case, the interquartile range shows highest values in the late Ypresian and Priabonian, and overall, variability tends to be greater in the post-Ypresian intervals compared to the earlier time bins. The number of septa shows a direct correlation with corallite spacing (rho = 0.84, $p = 0.029$).

## 4. Discussion

### 4.1. Morphological coral traits and their response to thermal stress: what we know from modern studies

In this section, we summarize key findings from the available literature on modern reef corals, focusing on how morphological traits (those that can be preserved and identified in fossil corals) respond to environmental disturbances, particularly thermal stress caused by rising ocean temperatures due to climate change. This stress can lead to coral bleaching, a process in which corals expel the symbiotic algae essential to their survival.

*Colony size*. According to some recent studies, larger coral colonies (over 30 cm) are generally more prone to bleaching due to heat stress, possibly because of higher metabolic demands or greater heat exposure. In contrast, smaller or juvenile corals (under 5 cm) tend to be more resistant to bleaching, likely due to their lower surface area-to-volume ratio and reduced exposure to stress, though they may be more susceptible to predation or physical damage (Burn et al., 2023; Winslow et al., 2024). Other authors, however, postulate that larger colonies, hosting more coral polyps, have more available energy and are more adapted to thrive in non-favourable conditions, being more tolerant to thermal stress than small colonies (Van Woesik et al., 2012; Darling et al., 2012). Larger colonies are also more prone to experiencing partial mortality due to stress or disturbances, whereas species with smaller colonies might be more likely to face complete colony loss (Darling et al., 2012). Despite these controversial interpretations, it is important to point out that thermal stress, if prolonged, can negatively affect coral growth and calcification rates leading to a reduction in overall size.

*Colony growth form (degree of branching)*. Many processes that determine the success of corals, and the ecosystem function they provide, are linked to colony morphology in a broad sense. According to Van Woesik et al. (2012), massive corals are more tolerant to thermal stress with respect to branching corals. According to Zawada et al. (2019), to which we refer for additional and specific references, traits such as volume compactness, surface complexity and top-heaviness can be used to track the response of corals. Colonies with low compactness (i.e., branching) show a higher bleaching and $pCO_2$ susceptibility with respect to more compact colonies (i.e., massive). High surface complexity (typical of colonies with bumpy surfaces) has also been linked to a high heat-induced bleaching susceptibility. Top-heaviness describes the vertical distribution of a colony's surface area and volume, representing a spectrum that ranges from encrusting and massive forms to laminar and tabular structures: top-heavy colonies, being higher in the water column are much more exposed to higher light levels and thus more susceptible to heat-induced bleaching. Low compactness is in general associated with a fast growth, with branching species growing much faster than massive species (Renema et al., 2016). Faster growth demands, however, greater energy investment, leading to the general agreement that branching and fast-growing corals are more sensitive to temperature anomalies (Loya et al., 2001; Pinzón et al., 2014; Denis et al., 2017; Raja et al., 2021).

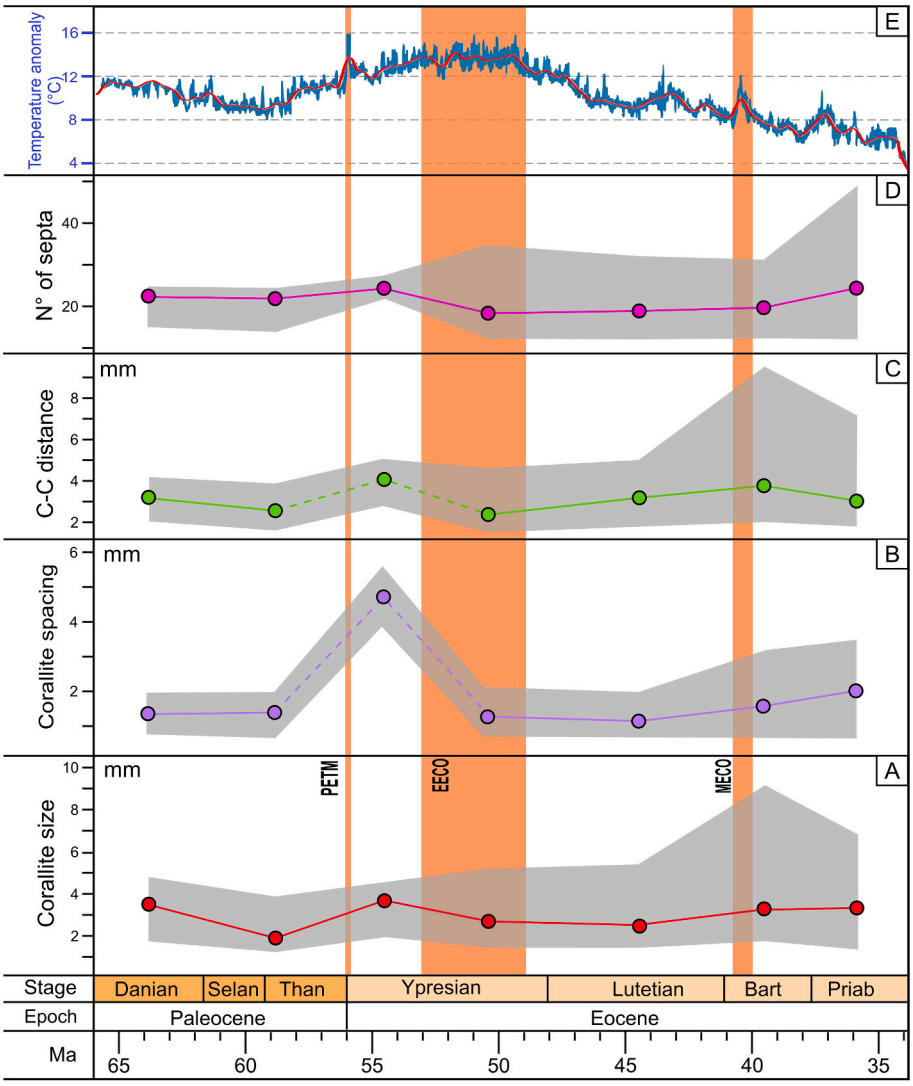


**Fig. 6.** Changes in corallite size, corallite spacing, distance between corallite centers (C–C distance) and number of septa across the Paleocene and Eocene. A) Median corallite size (red line with circles). B) Median corallite spacing (purple line with circles). C) Median C–C distance (green line with circles). D) Median number of septa (pink line with circles). E) Global temperature anomaly, from Westerhold et al., 2020). Gray areas indicate the variability across the median values. Dashed lines indicate time intervals with low sample size. Hyperthermal and warming events are highlighted: PETM (Paleocene-Eocene Thermal Maximum), EECO (Early Eocene Climatic Optimum), and MECO (Middle Eocene Climatic Optimum). (For interpretation of the references to colour in this figure legend, the reader is referred to the web version of this article.)

*Corallite integration*. Connections among strongly integrated polyps may enable the spread of harmful byproducts generated during the bleaching process. As a result, coral species with high polyp integration could be more susceptible to thermal stress and bleaching (Baird and Marshall, 2002; Swain et al., 2018). This trait can also be correlated with corallite spacing: according to van Woesik et al. (2012), a larger distance between corallites (i.e., colonies with a well-developed coenosteum) can be associated to a higher tolerance and recovery from thermal stress.

*Budding type*. The mode of budding (intracalicular vs. extracalicular) influences how light passes through the coral skeleton, thereby affecting the light absorption of coral symbionts and their susceptibility to climate disturbances. According to Raja et al. (2021), and reference therein, corals that exhibit extracalicular budding generally possess significantly greater light-scattering capabilities compared to those with intra-calicular budding but, at the same time, their late sexual maturity has also been related to population extinctions. The budding type is more difficult to interpret as a straightforward indicator of thermal stress resilience, as its effect on coral performance depends on a trade-off: while increased light availability may benefit photosynthesis, it can also lead to greater internal light stress at elevated temperatures, potentially increasing susceptibility to bleaching.

*Corallite size*. Smaller corallites are well adapted to capture light due to a greater surface area available for zooxanthellae, thus being often linked to increased reliance on photosymbiotic autotrophy. Species with larger corallites, having low surface-to-volume, tend to exhibit greater heterotrophic feeding and are less dependent on photosymbionts (Crabbe and Smith, 2006; Zapalski et al., 2017; Conti-Jerpe et al., 2020). Additionally, larger corallites support heterotrophic feeding under thermal stress, and can reduce mortality during symbiosis breakdown (Hughes and Grottoli, 2013). According to van Woesik et al. (2012), corallite size in an indicator of energy storage of individual coral polyps, with larger corallites able to store more energy and persist in more harsh environments than species with smaller corallites.

### 4.2. *Fossil evidence: Coral morphological trait responses during the early Paleogene hothouse and subsequent reef recovery*

Our results underline several changes in coral traits from the early

Paleocene to the end of the Eocene, encompassing the hothouse and warmhouse phases including their associated hyperthermal and warming events (Westerhold et al., 2020), and indicate that the response of coral traits during or shortly after the early Paleogene warming events does not always mirror the patterns observed in modern reefs under ongoing climate warming. In several cases, traits that are currently considered tolerant or resilient to thermal stress did not show a similar response in our analysis. The most suitable interval for comparison with modern warming is between the pre-PETM and the EECO, as it represents a phase of sustained global warming. A summary of our findings is shown in Fig. 7, which excludes the MECO. This event, although occurring within a warmhouse climate context, is characterised by relatively lower temperatures compared to the immediately preceding interval, making it less comparable to present-day warming trends.

To fully understand the response of coral traits during this time interval, it is also necessary to consider other driving mechanisms. These include: (a) changes in coral reef volume, recently reconstructed by Bosellini et al. (2025) for the early Paleogene in the Mediterranean region; (b) variations in reef sediment types, particularly the transition between carbonate and mixed carbonate-siliciclastic systems; and (c) the diversification of *Symbiodinium* zooxanthellae. These factors, together with temperature anomalies, $pCO_2$ and pH values, are illustrated in Fig. 8 and provide a broader context for interpreting the evolution of coral traits during this time.

Our data about colony size, expressed by colony width and height, positively correlate with the fact, underlined by some recent studies (Burn and Hoey, 2023; Winslow et al., 2024), that small colonies are more resistant to bleaching with respect to the larger ones as we document a decrease after the sharp and short hyperthermal event of the PETM in the early Ypresian and parallel with the beginning of the reef collapse. From the EECO colony size increased gradually until the MECO, then showed a more significant increase at the end of the Eocene, coinciding with reef recovery and the first radiation event of *Symbiodinium* zooxanthellae, thus testifying to much more favourable conditions for corals to calcify and produce carbonate (Fig. 2; Fig. 8). A small colony size has been recorded in the fossil record for the earliest Eocene coral assemblages (Zamagni et al., 2012) and for the EECO and post-EECO coral fauna from Friuli in northern Italy (Bosellini et al., 2022).

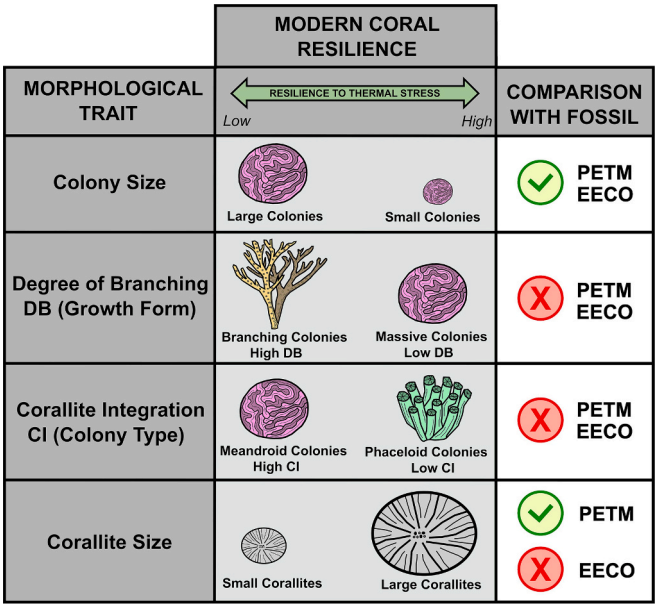


**Fig. 7.** Comparison of morphological traits linked to thermal stress resilience in modern corals and their correspondence with fossil coral assemblages from the PETM (Paleocene-Eocene Thermal Maximum) and EECO (Early Eocene Climatic Optimum). Green check marks indicate that the trait in the past responds accordingly to modern corals to thermal stress; the red cross indicate that the trait in the fossil record responded differently to modern corals to thermal stress. (For interpretation of the references to colour in this figure legend, the reader is referred to the web version of this article.)

Changes of colony growth forms (in terms of degree of branching) show a pattern opposite to what we would expect based on the modern response of coral growth forms to thermal stress (Fig. 7). Typically, branching colonies are considered less tolerant to thermal stress compared to massive forms. However, we observe an increase in the degree of branching after the PETM, during the EECO, and after the MECO. Interestingly, another increase occurs at the end of the Eocene, when global temperatures had already transitioned toward a coolhouse phase and coral reefs began to flourish again. In this case, the pattern is consistent with the modern response, but it does not occur during a warm phase.

This trait shows a strong correlation with the type of depositional setting: the degree of branching is positively associated with mixed siliciclastic-carbonate sediments ($r = 0.88$, $p = 0.0095$; rho $= 0.79$, $p = 0.041$), which became increasingly common from the late Ypresian onward (Fig. 8), and negatively associated with pure carbonate settings ($r = -0.88$, p $= 0.0095$; rho $= -0.79$, $p = 0.048$). This pattern can be explained by the fact that the high surface complexity of branching coral colonies enhances their resistance to sedimentation (Stafford-Smith and Ormond, 1992). In particular branching corals are known to be the most effective with respect to sediment clearance by passive removal as water flow between their branches helps dislodge and remove sediment particles (Sanders and Baron-Szabo, 2005 and references therein). In contrast, massive and encrusting corals are more susceptible to sediment accumulation, as their surfaces are more easily covered and they often lack efficient sediment-clearing mechanisms (Duckworth et al., 2017, for a review). Therefore, the observed increase in the degree of branching during the hothouse period, which contrasts with the response of modern corals under warming conditions, could reflect an adaptive strategy by reef corals to cope with increased sedimentation and turbidity in mixed carbonate-siliciclastic, possibly mesophotic, settings (Bosellini et al., 2024b and references therein).

Similarly to the degree of branching, the response of corallite integration, reflected in a variety of colony growth forms, in our dataset does not align with modern observations, which indicate that highly integrated colonies (e.g., hydonophoroid, meandroid, flabelloid) are generally less tolerant to thermal stress (Swain et al., 2018; Raja et al., 2021) (Fig. 7). Our results in fact show an increase of corallite integration during the hothouse (just after the PETM and EECO) and a decrease after the Lutetian during the cooling trend (Fig. 4). Our data show that corallite integration tends to correlate negatively with the reef volume (Fig. 8). At least during the early Paleogene, phaceloid, plocoid and cerioid colonies prevailed when reefs were more developed (early-middle Paleocene and late Eocene), whereas meandroid colonies were more abundant in absence of large reefs (Fig. 8).

As the potential resilience associated with budding type (i.e., intracalicular vs. extracalicular) in modern corals remains unclear, we cannot draw a direct comparison with fossil corals for this trait. Nevertheless, our data clearly show an increase in corals with intracalicular budding during the hothouse interval, paralleling the same pattern observed in meandroid corals, for which this budding type is typical.

Changes in corallite size indicate a clear increase in larger corallites immediately following the rapid thermal stress associated with the PETM. This pattern supports observations from modern corals, where larger corallites, being less reliant on photosymbiotic autotrophy, which is highly susceptible to damage during bleaching events, are linked to greater stress tolerance and a reduced risk of extinction (Crabbe and Smith, 2006; Zapalski et al., 2017; Conti-Jerpe et al., 2020; Raja et al., 2021) (Fig. 7). Corallite size decreased during the EECO, then gradually increased again toward the end of the Eocene. For the EECO, this pattern may be associated with an increase in branching corals, which are typically small-polyped, and with the pronounced presence of mixed carbonate-siliciclastic settings (Fig. 8). In general, a positive correlation

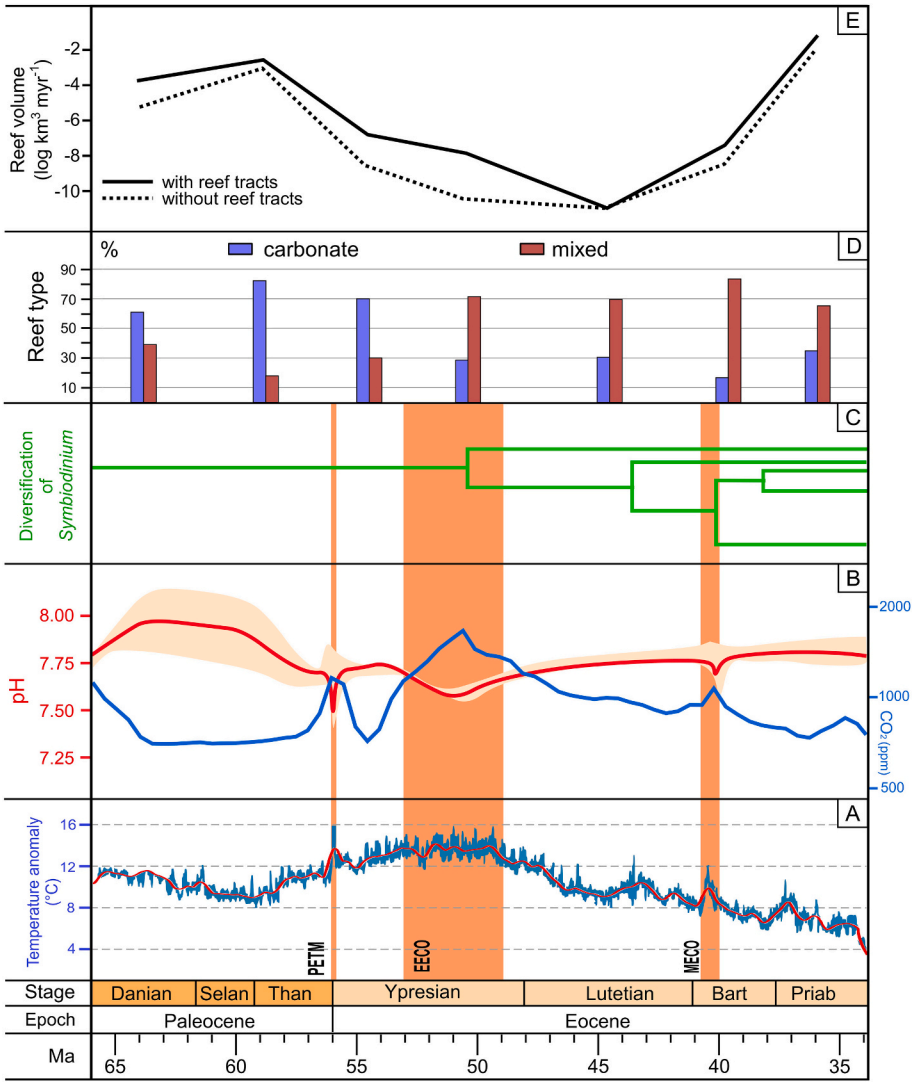


**Fig. 8.** Environmental and ecological trends across the Paleocene and Eocene, with emphasis on major hyperthermal events (PETM, EECO, MECO; shaded orange). A) Global temperature anomalies (°C) from Westerhold et al. (2020). B) Atmospheric $CO_2$ levels (blue line) (Whiteford et al., 2024) and surface ocean pH (red line) (Hönisch et al., 2023). C) Diversification of the symbiotic *Symbiodinium* dinoflagellate (Pochon et al., 2006). D) Reef sedimentary composition (% of carbonate vs mixed siliciclastic-carbonate systems). Carbonate-dominated in blue, mixed carbonate-siliciclastic in red. E) Values of estimated coral reef volume (log $km^3$ $myr^{-1}$), from Bosellini et al. (2025). (For interpretation of the references to colour in this figure legend, the reader is referred to the web version of this article.)

is documented with the data about reef volume and associated drivers (Fig. 8) as larger corallites are reported from both the early Paleocene and late Eocene.

Independent of the comparison with modern responses, which may be consistent in some cases and not in others (Fig. 7), our data on morphological traits can be used to trace changes in the structural composition of reef coral assemblages and to outline a trajectory from the Paleocene to the end of the Eocene (Fig. 9). This trajectory includes the transition from the well-developed Danian reefs to the equally developed upper Eocene reefs and spans a globally recognized reef crisis (Kiessling and Simpson, 2011; Scheibner and Speijer, 2008; Zamagni et al., 2012), which coincides with the hothouse phase extending from the PETM to the post-EECO interval. It also includes the shift, around the time of the EECO, from carbonate depositional environments to mixed carbonate-siliciclastic setting. Notably, the variability in dimensional parameters does not correlate with the number of measurements (or occurrences), suggesting that it may reflect genuine ecological variation rather than sampling bias.

In addition to the changes in the individual traits already described and discussed above, and synthetically illustrated in Fig. 9, it is possible to observe a trend from the EECO to the late Eocene (Bartonian-Priabonian) characterised by a diversification of coral assemblages. During the late Eocene we observe a remarkable increase in coral colony width and height, a variety of growth forms with a rapid rise in the degree of branching, and corallite size and spacing showing their highest variability, indicating greater morphological disparity. This trend likely reflects coral responses to global cooling, with more favourable conditions for both coral development and reef accretion which may have promoted diversification in growth strategies. In contrast, earlier intervals, particularly the post-PETM and EECO, show evidence of stress-related constraints on coral morphology and reef structure.

### 4.3. *Past vs. present: Interpreting ecological changes across geological and modern time scales*

Our study, along with the comparison between fossil and extant coral data, offers a valuable perspective for critically evaluating the fossil record as a potential analogue for present and future reef dynamics.

Understanding ecological change across geological and modern time scales is essential for assessing the resilience, adaptability, and

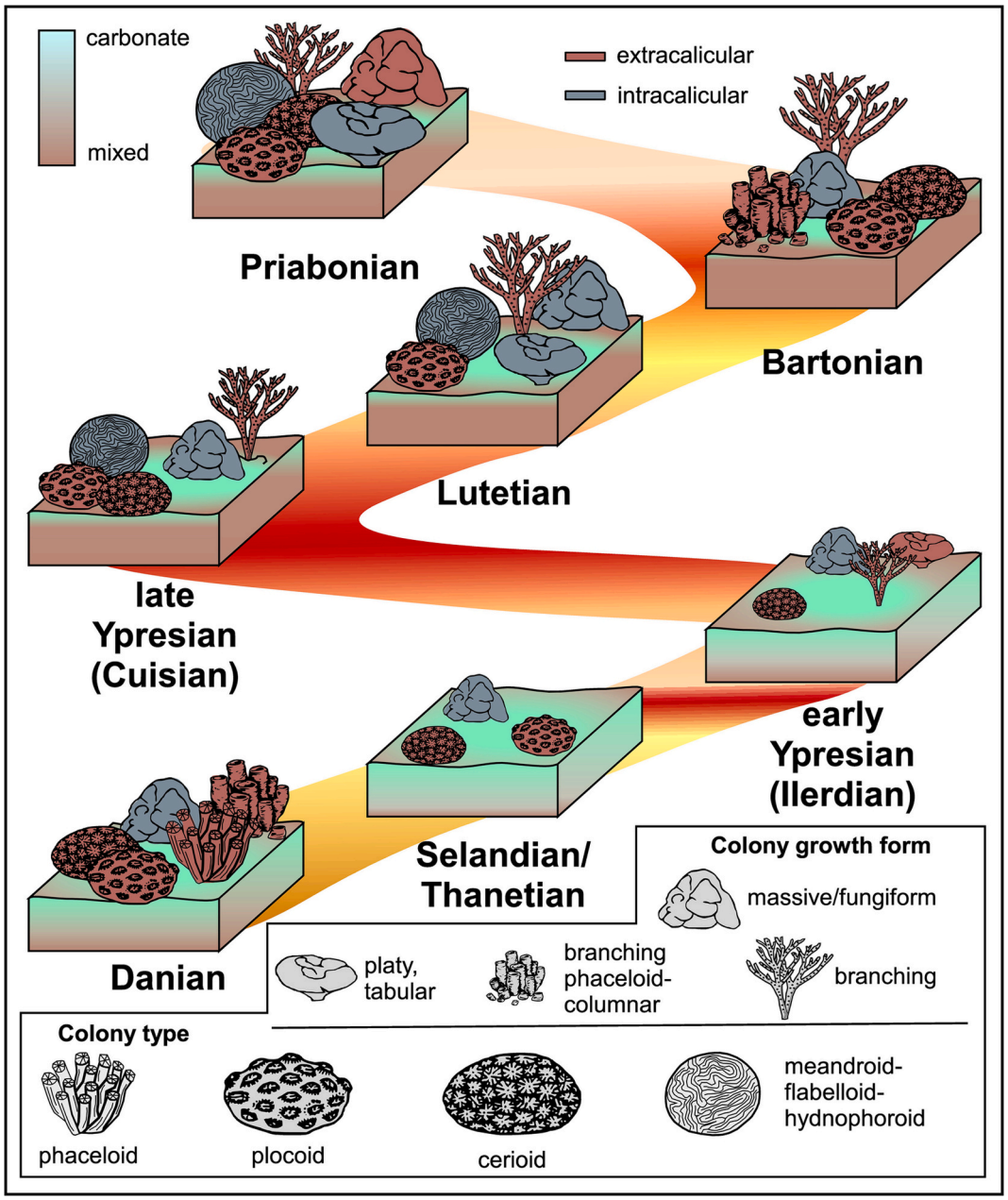


**Fig. 9.** Trajectories of coral morphological traits from the Paleocene to the Eocene (Danian to Priabonian). Block diagrams schematically show the temporal distribution and shifting dominance of colony-level traits, including growth form, colony type, and budding mode (intracalicular vs extracalicular). These trajectories are contextualized by depositional setting (carbonate vs mixed siliciclastic-carbonate systems) and coral frequency. A red-shaded background band indicates relative global warming intensity, with darker red tones marking peak hyperthermal conditions (e.g., PETM and EECO). (For interpretation of the references to colour in this figure legend, the reader is referred to the web version of this article.)

vulnerability of ecosystems to both natural processes and anthropogenic influences. The geological record provides long-term, low-resolution insights into natural rhythms, evolutionary processes, and climate-ecosystem feedbacks. It is undoubtedly the sole observational source that holds essential insights into how the climate system functions and how ecosystems like coral reefs responded in the past to climates significantly warmer than today (Pandolfi and Kiessling, 2014; Dee et al., 2019; Tierney et al., 2020). In contrast, modern observations offer high-resolution data over shorter periods, capturing the pace and magnitude of anthropogenic change.

The early Eocene time interval, and in particular the PETM hyperthermal event, have been used as a potential ancient analogue to the present-day anthropogenic-forced climate change (Tierney et al., 2022). The PETM witnessed a sharp increase in global temperatures, estimated to be between 5 and 8 °C, triggering profound environmental changes. These changes, however, occurred over a longer timescale (thousands of years), while rapid in geological terms, are still slower compared to the current human-driven warming (decades).

Bridging these geological and modern time scales, however, is challenging and requires overcoming differences in temporal resolution and data types. Comparing modern ecological responses to fossil (palaeoecological) responses to similar environmental stressors often reveals differences in magnitude, rate, or type of response. Nevertheless, these differences can yield valuable scientific insights and recognizing the strengths and limitations of each time scale is essential for building a comprehensive understanding of ecological change.

This is the case in our study, where the response of coral traits to past phases of warming and elevated levels of $CO_2$ does not always match

what is observed in the present day. Possible reasons for different responses can be attributed to several interrelated factors. A primary distinction lies in the rate and magnitude of change: contemporary shifts, such as climate warming, atmospheric $CO_2$ rise, and land-use transformation, are occurring at rates several orders of magnitude faster than most perturbations preserved in the geological record (IPCC, 2023). Such rapid environmental change may exceed the capacity for evolutionary or ecological adaptation, resulting in divergent outcomes even under comparable stressors (Quintero and Wiens, 2013). Additionally, modern ecosystems are subjected to a suite of novel, co-occurring stressors, including habitat fragmentation, invasive species, pollution, and overexploitation, that have no clear analogues in deep time (Jackson, 2008; Steffen et al., 2015; Chan et al., 2025). Differences in data resolution must be considered: fossil records are often temporally smoothed, potentially masking short-term ecological collapses or rapid recovery events (Kidwell and Flessa, 1995), whereas modern ecological data provide high-resolution temporal snapshots that can detect transient dynamics and early warning signals (Hughes et al., 2018). Sampling bias and the degree of fossil preservation have likely played a role, especially when considering morphological traits that are subject to subjective interpretation and closely tied to the mode of preservation. It should be also noted that the interpretation of coral ecological strategies in the early Paleogene is necessarily constrained by the geographic and preservational bias of the fossil record. Most quantitative trait data for Paleocene–Eocene scleractinian corals derive from the western Tethys–Mediterranean region, while comparable datasets from other coeval basins are still lacking. Consequently, inter-regional comparisons similar to those observed in modern coral assemblages (e.g., Fine et al., 2013; Evensen et al., 2021) cannot yet be performed. Future studies integrating morphological, ecological, and geochemical evidence from a wider range of regions will be essential to fully assess spatial patterns of coral resilience during early Paleogene climate perturbations.

Finally, when working with the fossil record, it is important to recognize that ancient reef systems may have developed under different boundary conditions and responded to distinct stressors or thresholds. This appears to be the case, at least in part, in our study: a reef crisis occurred during a time when reef corals did not experience a significant extinction event, despite this phase coinciding with a rise in sea surface temperatures and extremely high $pCO_2$ levels (Fig. 8). These conditions led to increased ocean acidification, enhanced weathering rates, elevated nutrient levels, and a low aragonite saturation state, all of which negatively impacted the ability of reef corals to optimize photoautotrophy and efficiently produce carbonate to build extensive reef structures (Zamagni et al., 2012; Bosellini et al., 2025).

Despite these challenges, corals appeared remarkably resilient, developing adaptive strategies that allowed them to survive and diversify under these stressed and harsh conditions, often by finding refuges in mesophotic, mixed carbonate-siliciclastic environments (Dimitrijević et al., 2024). The resilience of modern coral traits is strongly influenced by the impact of global warming on photosymbiosis, a key factor in reef-building capacity. Therefore, we propose that the long-term decoupling between reef coral diversity and reef proliferation in the Paleocene and Eocene of the Mediterranean region may have played a significant role in shaping the coral trait patterns we observe.

Interestingly, a positive correlation with modern reef-building traits was documented during the Late Devonian reef collapse which, unlike the early Paleogene crisis, was associated with a major mass extinction event (Bridge et al., 2022). During the reef peak in the Givetian, coral assemblages were dominated by small corallites and high corallite integration, traits typically linked to reef-building and considered proxies for photosynthetic efficiency. Many of the species exhibiting these traits went extinct at the end of the Givetian, at the onset of the reef crisis, after which corals with large corallites and low corallite integration became more prevalent. In contrast, during the PETM reef crisis, we observe a different trend: there is a marked increase in corallite integration, commonly associated with enhanced photosynthetic capacity, and only a partial increase in corallite size, which subsequently declines after the PETM.

As a concluding remark, we emphasize that when modern reef responses differ from fossil responses to seemingly similar environmental stressors, it is not necessarily contradictory. Rather, it underscores the importance of context, temporal scale, and ecological complexity. Recognizing these differences enables scientists to refine predictions, identify vulnerable systems, and design more effective strategies for mitigation and adaptation in a rapidly changing world.

## 5. Conclusions

Global climate change is expected to drive the degradation of modern coral reefs. Because ancient reefs have experienced multiple crisis events, often slowing down or ceasing during periods of climatic instability, the fossil record offers a valuable archive for understanding how coral reef ecosystems have responded to comparable environmental pressures in Earth's history. In this context, coral reefs can be viewed not only as three-dimensional, framework-building ecosystems, but also as assemblages of hypercalcifying organisms with individual traits and evolutionary trajectories.

In this study, we used the PalEoCoralTraits (PECT) dataset to analyse a suite of morphological traits in reef-building corals from the Mediterranean region during the early Paleogene, spanning from the early Paleocene through the end of the Eocene. Our analysis includes the reef crisis and subsequent recovery phase. The main findings are as follows:

- Coral trait responses to early Paleogene warming events (PETM and EECO) do not consistently align with patterns observed in modern reefs under ongoing climate change. While traits such as colony size and, to some extent, corallite size (during the PETM) show resilience comparable to modern responses, growth form (degree of branching) and corallite integration exhibit divergent trajectories during both hyperthermal events.
- During the long-term reef crisis (PETM–Lutetian), coral traits follow distinct patterns: colony size remains small; the degree of branching increases up to the EECO, then declines during the Lutetian but stays lower than in the recovery phase; corallite integration peaks in the Lutetian; budding type values decline due to increased intracalicular budding; and corallite size rises after the PETM, then decreases.
- In the reef recovery phase (Bartonian–Priabonian), colony size and branching increase, while corallite integration declines. Budding type values increase, driven by a shift toward extracalicular budding. Corallite size slightly increases after the Lutetian, and both corallite spacing and septal number show a rising trend.
- The increase in coral branching following the PETM and throughout the Eocene correlates positively with the expansion of mixed siliciclastic–carbonate depositional settings over purely carbonate ones. This trend, differing from modern coral responses to warming, may indicate an adaptive strategy to cope with increased sedimentation and turbidity in mixed, possibly mesophotic, environments.
- The morphological trajectories observed suggest a broader ecological restructuring of coral assemblages in response to early Paleogene environmental changes, marked by an overall increase in morphological disparity from the EECO to the late Eocene. Global cooling and the diversification of *Symbiodinium* zooxanthellae may have fostered more favourable conditions for coral development and reef accretion, promoting diversification in growth strategies.
- Differences between the responses of coral traits to warming phases in our fossil data and those in modern systems may result from several factors: the rate and magnitude of climatic change, the presence of novel Anthropocene stressors, differences in data and temporal resolution, sampling biases, and the degree of fossil preservation. Additionally, the long-term decoupling between coral diversity and reef development during the Paleocene and Eocene in the

Mediterranean region may reflect distinct boundary conditions, stressors, or ecological thresholds compared to today.
- While the fossil record cannot serve as a direct predictive analogue for the future of modern reefs, it provides critical insights into collapse thresholds, recovery patterns, and coral adaptability under past climate stress events.

Supplementary data to this article can be found online at https://doi.org/10.1016/j.palaeo.2025.113472.

## CRediT authorship contribution statement

**Francesca R. Bosellini:** Writing – review & editing, Writing – original draft, Visualization, Validation, Supervision, Software, Resources, Project administration, Methodology, Investigation, Funding acquisition, Formal analysis, Data curation, Conceptualization. **Luca Mariani:** Writing – review & editing, Writing – original draft, Visualization, Validation, Supervision, Software, Resources, Methodology, Investigation, Formal analysis, Data curation, Conceptualization. **Andrea Benedetti:** Writing – review & editing, Visualization, Validation, Supervision, Software, Methodology, Investigation, Formal analysis, Data curation.

## Declaration of generative AI and AI-assisted technologies in the writing process

During the preparation of this work the authors used ChatGPT (OpenAI) in order to support the refinement of narrative structure, clarity of expression, and adherence to journal formatting guidelines. After using this tool, the authors reviewed and edited the content as needed and take full responsibility for the content of the publication.

## Declaration of competing interest

The authors declare that they have no known competing financial interests or personal relationships that could have appeared to influence the work reported in this paper.

## Acknowledgments

We thank the following museums for granting us access to their collections and for loaning coral specimens for this study: Museo Friulano di Storia Naturale (Udine), Museo di Storia Naturale dell'Università di Firenze, Museo dell'Università di Padova, Geologische Bundesanstalt Wien, Museo di Storia Naturale dell'Università di Pisa, Museo di Storia Naturale di Venezia, Museo Civico "G.Zannato", Montecchio Maggiore (VI).

The authors thank Prof. M. Zapalski, two anonymous reviewers, and the editor (L. Angiolini), for their constructive remarks. This research is funded by European Union – Next Generation EU PRIN MUR 2022WEZE44 to C. Bottini "Conservation of life on Earth: the fossil record as an unparalleled archive of ecological and evolutionary responses to past warming events".

## Data availability

All the data used in this study are available at Zenodo repository: https://doi.org/10.5281/zenodo.17543276

## References

Baird, A.H., Marshall, P.A., 2002. Mortality, growth and reproduction in scleractinian corals following bleaching on the Great Barrier Reef. Mar. Ecol. Prog. Ser. 237, 133–141. https://doi.org/10.3354/meps237133.

Benedetti, A., Papazzoni, C.A., Bosellini, F.R., 2024a. Unparallel resilience of shallow-water tropical calcifiers (foraminifera and reef scleractinian corals) during the early Paleogene global warming intervals. Palaeogeogr. Palaeoclimatol. Palaeoecol. 651, 112393. https://doi.org/10.1016/j.palaeo.2024.112393.

Benedetti, A., Papazzoni, C.A., Bosellini, F., Giusberti, L., Fornaciari, E., 2024b. High diversity larger foraminiferal assemblages from the post-EECO of Collio (Friuli-Venezia Giulia, northern Italy), calibrated with calcareous nannoplankton biozones. Palaeoworld 33, 492–503. https://doi.org/10.1016/j.palwor.2023.01.013.

Bosellini, F.R., Benedetti, A., Budd, A.F., Papazzoni, C.A., 2022. A coral hotspot from a hot past: the EECO and post-EECO rich reef coral fauna from Friuli (Eocene, NE Italy). Palaeogeogr. Palaeoclimatol. Palaeoecol. 607, 111284. https://doi.org/10.1016/j.palaeo.2022.111284.

Bosellini, F.R., Benedetti, A., Kiessling, W., 2024a. Mediterranean reef coral diversity and reef volume in the Paleocene and Eocene [Dataset]. Zenodo. https://doi.org/10.5281/zenodo.12912501.

Bosellini, F.R., Vescogni, A., Briguglio, A., Piazza, M., Papazzoni, C.A., Silvestri, G., Morsilli, M., 2024b. Growth and demise of mesophotic coral buildups in a fan-delta system during the Late Oligocene Warming Event (Tertiary Piedmont Basin, NW Italy). Palaeogeogr. Palaeoclimatol. Palaeoecol. 649, 112330. https://doi.org/10.1016/j.palaeo.2024.112330.

Bosellini, F.R., Benedetti, A., Kiessling, W., 2025. Minor coral diversity loss but long-lasting coral reef crises in the early Paleogene hothouse. Paleoceanogr. Paleoclimatol. 40. https://doi.org/10.1029/2024PA004985 e2024PA004985.

Bridge, T.C.L., Baird, A.H., Pandolfi, J.M., McWilliam, M.J., Zapalski, M.K., 2022. Functional consequences of Palaeozoic reef collapse. Sci. Rep. 12, 1386. https://doi.org/10.1038/s41598-022-05154-6.

Burn, D., Hoey, A.S., Matthews, S., Harrison, H.B., Pratchett, M.S., 2023. Differential bleaching susceptibility among coral taxa and colony sizes, relative to bleaching severity across Australia's Great Barrier Reef and Coral Sea Marine Parks. Mar. Poll. Bull. 191, 114907. https://doi.org/10.1016/j.marpolbul.2023.114907.

Carpenter, K.E., Abrar, M., Aeby, G., Aronson, R.B., Banks, S., Bruckner, A., et al., 2008. One-Third of Reef-Building Corals Face Elevated Extinction Risk from climate Change and Local Impacts. Science 321, 560–563. https://doi.org/10.1126/science.1159196.

Chan, Y.K.S., Ang, A.C.F., Choo, M., Oh, R.E., Morgan, K.M., Todd, P.A., O'Leary, M.J., Huang, D., 2025. Holocene coral assemblages reveal similarities to living communities in Singapore's urban reef environment. Palaeogeogr. Palaeoclimatol. Palaeoecol. 669, 112930. https://doi.org/10.1016/j.palaeo.2025.112930.

Conti-Jerpe, I.E., Thompson, P.D., Wong, C.W.M., Oliveira, N.L., Duprey, N.N., Moynihan, M.A., Baker, D.M., 2020. Trophic strategy and bleaching resistance in reef-building corals. Sci. Adv. 6, eaaz5443. https://doi.org/10.1126/sciadv.aaz5443.

Crabbe, M.J.C., Smith, D.J., 2006. Modelling variations in corallite morphology of *Galaxea fascicularis* coral colonies with depth and light on coastal fringing reefs in the Wakatobi Marine National Park (S.E.Sulawesi, Indonesia). Comput. Biol. Chem. 30, 155–159. https://doi.org/10.1016/j.compbiolchem.2005.11.004.

Darling, E.S., Alvarez-Filip, L., Oliver, T.A., McClanahan, T.R., Côté, I.M., 2012. Evaluating life-history strategies of reef corals from species traits. Ecol. Lett. 15, 1378–1386. https://doi.org/10.1111/j.1461-0248.2012.01861.x.

Dee, S.G., Torres, M.A., Martindale, R.C., Weiss, A., DeLong, K.L., 2019. The Future of Reef Ecosystems in the Gulf of Mexico: Insights from coupled climate Model Simulations and Ancient Hot-House Reefs. Front. Mar. Sci. 6, 691. https://doi.org/10.3389/fmars.2019.00691.

Denis, V., Ribas-Deulofeu, L., Sturaro, N., Kuo, C.-Y., Chen, C.A., 2017. A functional approach to the structural complexity of coral assemblages based on colony morphological features. Sci. Rep. 7, 9849. https://doi.org/10.1038/s41598-017-10334-w.

Dimitrijević, D., Raja, N.B., Kiessling, W., 2023. Corallite sizes of reef corals: decoupling of evolutionary and ecological trends. Paleobiology 50, 43–53. https://doi.org/10.1017/pab.2023.28.

Dimitrijević, D., Santodomingo, N., Kiessling, W., 2024. Reef refugia in the aftermath of past episodes of global warming. Coral Reefs 43, 1431–1442. https://doi.org/10.1007/s00338-024-02548-y.

Duckworth, A., Giofre, N., Jones, R., 2017. Coral morphology and sedimentation. Mar. Poll. Bull. 125 (1–2), 289–300. https://doi.org/10.1016/j.marpolbul.2017.08.036.

Eddy, T.D., Lam, V.W.Y., Reygondeau, G., Cisneros-Montemayor, A.M., Greer, K., Palomares, L.M.D., Bruno, J.F., Ota, Y., Cheung, W.W.L., 2021. Global decline in capacity of coral reefs to provide ecosystem services. One Earth 4 (9), 1278–1285. https://doi.org/10.1016/j.oneear.2021.08.016.

Evensen, N.R., Fine, M., Perna, G., Voolstra, C.R., Barshis, D.J., 2021. Remarkably high and consistent tolerance of a Red Sea coral to acute and chronic thermal stress exposures. Limnol. Oceanogr. 66, 1718–1729. https://doi.org/10.1002/lno.11715.

Fine, M., Gildor, H., Genin, A., 2013. A coral reef refuge in the Red Sea. Glob. Change Biol. 19, 3640–3647. https://doi.org/10.1111/gcb.12356.

Fontoura, L., Zawada, K.J.A., D'agata, S., Álvarez-Noriega, M., Baird, A.H., Boutros, N., Dornelas, M., Luiz, O.J., Madin, J.S., Maina, J.M., Pizarro, O., Torres-Pulliza, D., Woods, R.M., Madin, E.M.P., 2020. Climate-driven shift in coral morphological structure predicts decline of juvenile reef fishes. Glob. Change Biol. 26, 557–567. https://doi.org/10.1111/gcb.14911.

Hoegh-Guldberg, O., Mumby, P.J., Hooten, A.J., Steneck, R.S., Greenfield, P., Gomez, E., Harvell, C.D., Sale, P.F., Edwards, A.J., Caldeira, K., Knowlton, N., Eakin, C.M., Prieto-Iglesias, R., Muthiga, N., Bradbury, R.H., Dubi, A., Hatziolos, M.E., 2007. Coral Reefs under Rapid climate Change and Ocean Acidification. Science 318 (5857), 1737–1742. https://doi.org/10.1126/science.1152509.

Hönisch, B., Royer, D.L., Breecker, D.O., Polissar, P.J., Bowen, G.J., Henehan, M.J., et al., 2023. Toward a Cenozoic history of atmospheric $CO_2$. Science 382 (6675), eadi5177. https://doi.org/10.1126/science.adi5177.

Hughes, A.D., Grottoli, A.G., 2013. Heterotrophic compensation: a possible mechanism for resilience of coral reefs to global warming or a sign of prolonged stress? PloS One 8, e81172. https://doi.org/10.1371/journal.pone.0081172.

Hughes, T.P., Barnes, M.L., Bellwood, D.R., Cinner, J.E., Cumming, G.S., Jackson, J.B.C., Kleypas, J., van de Leemput, I.A., Lough, J.M., Morrison, T.H., Palumbi, S.R., van Nes, E.H., Scheffer, M., 2017a. Coral reefs in the Anthropocene. Nature 546, 82–90. https://doi.org/10.1038/nature22901.

Hughes, T.P., Kerry, J.T., Álvarez-Noriega, M., Álvarez-Romero, J.G., Anderson, K.D., Baird, A.H., et al., 2017b. Global warming and recurrent mass bleaching of corals. Nature 543, 373–377. https://doi.org/10.1038/nature21707.

Hughes, T.P., Kerry, J.T., Baird, A.H., Connolly, S.R., Dietzel, A., Eakin, C.M., Heron, S. F., Hoey, A.S., Hoogenboom, M.O., Liu, G., McWilliam, M.J., Pears, R.J., Pratchett, M.S., Skirving, W.J., Stella, J.S., Torda, G., 2018. Global warming transforms coral reef assemblages. Nature 556, 492–496. https://doi.org/10.1038/s41586-018-0041-2.

Inglis, G.N., Bragg, F., Burls, N.J., Cramwinckel, M.J., Evans, D., Foster, G.L., Huber, M., Lunt, D.J., Siler, N., Steinig, S., Tierney, J.E., Wilkinson, R., Anagnostou, E., de Boer, A.M., Jones, T.D., Edgar, K.M., Hollis, C.J., Hutchinson, D.K., Pancost, R.D., 2020. Global mean surface temperature and climate sensitivity of the Early Eocene Climatic Optimum (EECO), Paleocene–Eocene Thermal Maximum (PETM), and latest Paleocene. Climate of the Past 16 (5), 1953–1968. https://doi.org/10.5194/cp-16-1953-2020.

IPCC, 2022. Climate Change 2022: Impacts, Adaptation, and Vulnerability. Cambridge University Press. https://doi.org/10.1017/9781009325844.

IPCC, 2023. Climate Change 2023: Synthesis Report. Contribution of Working Groups I, II and III to the Sixth Assessment Report of the Intergovernmental Panel on Climate Change. IPCC, Geneva. https://www.ipcc.ch/report/sixth-assessment-report-synthesis-report/.

Jackson, J.B.C., 2008. Ecological extinction and evolution in the brave new ocean. Proc. Natl. Acad. Sci. U. S. A. 105, 11458–11465. https://doi.org/10.1073/pnas.0802812105.

Kidwell, S.M., Flessa, K.W., 1995. The quality of the fossil record: Populations, species, and communities. Annu. Rev. Ecol. Syst. 26, 269–299. http://www.jstor.org/stable/2097208.

Kiessling, W., Simpson, C., 2011. On the potential for ocean acidification to be a general cause of ancient reef crises. Glob. Chang. Biol. 17 (1), 56–67. https://doi.org/10.1111/j.1365-2486.2010.02204.x.

Loya, Y., Sakai, K., Yamazato, K., Nakano, Y., Sambali, H., van Woesik, R., 2001. Coral bleaching: the winners and the losers. Ecol. Lett. 4 (2), 122–131. https://doi.org/10.1046/j.1461-0248.2001.00203.x.

Luciani, V., Fornaciari, E., Papazzoni, C.A., Dallanave, E., Giusberti, L., Stefani, C., Amante, E., 2020. Integrated stratigraphy at the Bartonian-Priabonian transition: Correlation between shallow benthic and calcareous plankton zones (Varignano section, northern Italy). GSA Bull. 132, 495–520. https://doi.org/10.1130/B35169.1.

Madin, J.S., Anderson, K.D., Andreasen, M.H., Bridge, T.C.L., Cairns, S.D., Connolly, S.R., Darling, E.S., Diaz, M., Falster, D.S., Franklin, E.C., Gates, R.D., Harmer, A.M.T., Hoogenboom, M.O., Huang, D., Keith, S.A., Kosnik, M.A., Kuo, C.-Y., Lough, J.M., Lovelock, C.E., Luiz, O., Martinelli, J., Mizerek, T., Pandolfi, J.M., Pochon, X., Pratchett, M.S., Putnam, H.M., Roberts, T.E., Stat, M., Wallace, C.C., Widman, E., Baird, A.H., 2016. The Coral Trait Database, a curated database of trait information for coral species from the global oceans. Sci. Data 3, 160017. https://doi.org/10.1038/sdata.2016.17.

McInerney, F.A., Wing, S.L., 2011. The Paleocene-Eocene thermal Maximum: a Perturbation of carbon cycle, climate, and biosphere with implications for the future. Annu. Rev. Earth Planet. Sci. 39, 489–516. https://doi.org/10.1146/annurev-earth-040610-133431.

Pandolfi, J.M., Kiessling, W., 2014. Gaining insights from past reefs to inform understanding of coral reef response to global climate change. COSUST 7, 52–58. https://doi.org/10.1016/j.cosust.2013.11.020.

Pandolfi, J.M., Bradbury, R.H., Sala, E., Hughes, T.P., Bjorndal, K.A., Cooke, R.G., McArdle, D., McClenachan, L., Newman, M.J., Paredes, G., Warner, R.R., Jackson, J. B., 2003. Global trajectories of the long-term decline of coral reef ecosystems. Science 301, 955–958. https://doi.org/10.1126/science.1085706.

Papazzoni, C.A., Fornaciari, B., Giusberti, L., Simonato, M., Fornaciari, E., 2023. A new definition of the Paleocene Shallow Benthic zones (SBP) by means of larger foraminiferal biohorizons, and their calibration with calcareous nannofossil biostratigraphy. Micropaleontology 69 (4), 363–400. https://doi.org/10.47894/mpal.69.4.02.

Pinzón, C.J.H., Dornberger, L., Beach-Letendre, J., Weil, E., Mydlarz, L.D., 2014. The link between immunity and life history traits in scleractinian corals. PeerJ 2, e628. https://doi.org/10.7717/peerj.628.

Pochon, X., Montoya-Burgos, J.I., Stadelmann, B., Pawlowski, J., 2006. Molecular phylogeny, evolutionary rates, and divergence timing of the symbiotic dinoflagellate genus *Symbiodinium*. Mol. Phylogenet. Evol. 38, 20–30. https://doi.org/10.1016/j.ympev.2005.04.028.

Quintero, I., Wiens, J.J., 2013. Rates of projected climate change dramatically exceed past rates of climatic niche evolution among vertebrate species. Ecol. Lett. 16, 1095–1103. https://doi.org/10.1111/ele.12144.

Rae, J.W.B., Zhang, Y.G., Liu, X., Foster, G.L., Stoll, H.M., Whiteford, R.D.M., 2021. Atmospheric $CO_2$ over the past 66 million years from marine archives. Annu. Rev. Earth Planet. Sci. 49 (1), 599–631. https://doi.org/10.1146/annurev-earth-082420-063026.

Raja, N.B., Lauchstedt, A., Pandolfi, J.M., Kim, S.W., Budd, A.F., Kiessling, W., 2021. Morphological traits of reef corals predict extinction risk but not conservation status. Glob. Ecol. Biogeogr. 30, 1597–1608. https://doi.org/10.1111/geb.13321.

Raja, N.B., Dimitrijević, D., Krause, M.C., Kiessling, W., 2022. Ancient Reef Traits, a database of trait information for reef-building organisms over the Phanerozoic. Sci. Data 9, 425. https://doi.org/10.1038/s41597-022-01486-0.

Renema, W., Bellwood, D.R., Braga, J.C., Bromfield, K., Hall, R., Johnson, K.G., et al., 2008. Hopping hotspots: Global shifts in marine biodiversity. Science 321 (5889), 654–657. https://doi.org/10.1126/science.1155674.

Renema, W., Pandolfi, J.M., Kiessling, W., Bosellini, F.R., Klaus, J., Korpanty, C., Rosen, B.R., Santodomingo, N., Wallace, C.C., Webster, J.M., Johnson, K.G., 2016. Are coral reefs victims of their own past success? Sci. Adv. 2, e1500850. https://doi.org/10.1126/sciadv.1500850.

Sanders, D., Baron-Szabo, R.C., 2005. Scleractinian assemblages under sediment input: their characteristics and relation to the nutrient input concept. Palaeogeogr. Palaeoclimatol. Palaeoecol. 216, 139–181. https://doi.org/10.1016/j.palaeo.2004.10.008.

Scheibner, C., Speijer, R.P., 2008. Late Paleocene-early Eocene Tethyan carbonate platform evolution. A response to long- and short-term paleoclimatic change. Earth Sci. Rev. 90 (3–4), 71–102. https://doi.org/10.1016/j.earscirev.2008.07.002.

Scotese, C.R., Song, H., Mills, B.J.W., van der Meer, D.G., 2021. Phanerozoic paleotemperatures: the Earth's changing climate during the last 540 million years. Earth Sci. Rev. 215, 103503. https://doi.org/10.1016/j.earscirev.2021.103503.

Serra-Kiel, J., Hottinger, L., Caus, E., Drobne, K., Ferr'andez, C., Jauhri, A.K., Less, G., Pavlovec, R., Pignatti, J., Sams'o, J.M., Schaub, H., Sirel, E., Strougo, A., Tambareau, Y., Tosquella, J., Zakrevskaya, E., 1998. Larger foraminiferal biostratigraphy of the Tethyan Paleocene and Eocene. Bull. Soc. Geol. Fr. 169, 281–299.

Serra-Kiel, J., Vicedo, V., Baceta, J.I., Bernaola, G., Robador, A., 2020. Paleocene Larger Foraminifera from the Pyrenean Basin with a recalibration of the Paleocene Shallow Benthic Zone. Geol. Acta 18 (8), 1–70.

Simpson, C., Kiessling, W., Mewis, H., Baron-Szabo, R.C., Müller, J., 2011. Evolutionary diversification of reef corals: a comparison of the molecular and fossil records. Evolution 65 (11), 3274–3284. https://doi.org/10.1111/j.1558-5646.2011.01365.x.

Speijer, R.P., Pälike, H., Hollis, C.J., Hooker, J.J., Ogg, J.G., 2020. Chapter 28 – The Paleogene Period. In: Gradstein, F.M., Ogg, J.G., Schmitz, M.D., Ogg, G.M. (Eds.), Geologic Time Scale 2020. Elsevier, Amsterdam, pp. 1087–1140.

Stafford-Smith, M., Ormond, R., 1992. Sediment-rejection mechanisms of 42 species of Australian scleractinian corals. Mar. Freshw. Res. 43, 683–705. https://doi.org/10.1071/MF9920683.

Steffen, W., Richardson, K., Rockström, J., Cornell, S.E., Fetzer, I., Bennett, E.M., Biggs, R., Carpenter, S.R., De Vries, W., De Witt, C.A., Folke, C., Gerten, D., Heinke, J., Mace, G.M., Persson, L.M., Ramanathan, V., Reyers, B., Sörlin, S., 2015. Planetary boundaries: Guiding human development on a changing planet. Science 347, 1259855. https://doi.org/10.1126/science.1259855.

Swain, T.D., Bold, E.C., Osborn, P.C., Baird, A.H., Westneat, M.W., Backman, V., Marcelino, L.A., 2018. Physiological integration of coral colonies is correlated with bleaching resistance. Mar. Ecol. Progress Series 586, 1–10. https://doi.org/10.3354/meps12445.

Tierney, J.E., Poulsen, C.J., Montañez, I.P., Bhattacharya, T., Feng, R., Ford, H.L., Hönisch, B., Inglis, G.N., Petersen, S.V., Sagoo, N., Tabor, C.R., Thirumalai, K., Zhu, J., Burls, N.J., Foster, G.L., Goddéris, Y., Huber, B.T., Ivany, L.C., Turner, S.K., Lunt, D.J., McElwain, J.C., Mills, B.J.W., Otto-Bliesner, B.L., Ridgwell, A., Zhang, Y. G., 2020. Past climates inform our future. Science 370. https://doi.org/10.1126/science.aay3701 eaay3701.

Tierney, J.E., Zhu, J., Li, M., Ridgwell, A., Hakim, G.J., Poulsen, C.J., Whiteford, R.D.M., Rae, J.W.B., Kump, L.R., 2022. Spatial patterns of climate change across the Paleocene-Eocene thermal Maximum. Proc. Natl. Acad. Sci. U. S. A. 119 (42), e2205326119. https://doi.org/10.1073/pnas.2205326119.

van Woesik, R., Franklin, E.C., O'Leary, J., McClanahan, T.R., Klaus, J.S., Budd, A.F., 2012. Hosts of the plio-pleistocene past reflect modern-day coral vulnerability. Proc. R. Soc. B 279, 2448–2456. https://doi.org/10.1098/rspb.2011.2621.

Weiss, A.M., Martindale, R.C., 2019. Paleobiological traits that determined Scleractinian coral survival and proliferation during the late Paleocene and early Eocene hyperthermals. Paleoceanogr. Paleoclimatol. 34 (2), 252–274. https://doi.org/10.1029/2018PA003398.

Westerhold, T., Marwan, N., Drury, A.J., Liebrand, D., Agnini, C., Anagnostou, E., Barnet, J.S.K., Bohaty, S.M., De Vleeschouwer, D., Florindo, F., Frederichs, T., Hodell, D.A., Holbourn, A.E., Kroon, D., Lauretano, V., Littler, K., Lourens, L.J., Lyle, M., Palike, H., Rohl, U., Tian, J., Wilkens, R.H., Wilson, P.A., Zachos, J.C., 2020. An astronomically dated record of Earth's climate and its predictability over the last 66 million years. Science 369, 1383–1387. https://doi.org/10.1126/science.aba6853.

Whiteford, R., Heaton, T.J., Henehan, M.J., Anagnostou, E., Jurikova, H., Foster, G.L., Rae, J.W.B., 2024. Reconstruction of Cenozoic $\delta^{11}B_{sw}$ using a Gaussian process. Paleoceanogr. Paleoclimatol. 39. https://doi.org/10.1029/2023PA004769 e2023PA004769.

Winslow, E.M., Speare, K.E., Adam, T.C., Burkepile, D.E., Hench, J.L., Lenihan, H.S., 2024. Corals survive severe bleaching event in refuges related to taxa, colony size, and water depth. Sci. Rep. 14, 9006. https://doi.org/10.1038/s41598-024-58980-1.

Yasuhara, M., Huang, H.H.M., Reuter, M., Tian, S.Y., Cybulski, J.D., O'Dea, A., Mamo, B. L., Cotton, L.J., Martino, E.D., Feng, R., Tabor, C.R., Reygondeau, G., Zhao, Q., Warne, M.T., Aye, K.K., Zhang, J., Chao, A., Wei, C.L., Condamine, F.L., Kocsis, Á., Kießling, W., Costello, M.J., Tittensor, D.R., Chaudhary, C., Rillo, M.C., Yukidoi, H., Dong, Y.W., Cronin, T.M., Saupe, E.E., Lotze, H.K., Johnson, K.G., Renema, W., Pandolfi, J.M., Harzhauser, M., Jackson, J.B., Hong, Y., 2022. Hotspots of Cenozoic Tropical Marine Biodiversity. In: Hawkins, S.J., Allcock, A.L., Todd, P.A., Swearer, S. E., Byrne, M., Firth, L.B., et al. (Eds.), Oceanography and Marine Biology: An Annual

Review 60. Taylor & Francis, pp. 243–300. https://doi.org/10.1201/9781003288602-5.

Zamagni, J., Mutti, M., Košir, A., 2012. The evolution of mid Paleocene–early Eocene coral communities: how to survive during rapid global warming. Palaeogeogr. Palaeoclimatol. Palaeoecol. 317–318, 48–65. https://doi.org/10.1016/j.palaeo.2011.12.010.

Zapalski, M.K., Nowicki, J., Jakubowicz, M., Berkowski, B., 2017. Tabulate corals across the Frasnian/Famenian boundary: architectural turnover and its possible relation to ancient photosymbiosis. Palaeogeogr. Palaeoclimatol. Palaeoecol. 487, 416–429. https://doi.org/10.1016/j.palaeo.2017.09.028.

Zawada, K.J.A., Madin, J.S., Baird, A.H., Bridge, T.C.L., Dornelas, M., 2019. Morphological traits can track coral reef responses to the Anthropocene. Funct. Ecol. 33, 962–975. https://doi.org/10.1111/1365-2435.13358.